JACS
JOURNAL OF THE AMERICAN CHEMICAL SOCIETY

Communication

pubs.acs.org/JACS

Advancing Drug Formulation Additives toward Precision Additives with Release Mediating Peptide Interlayer

Sebastian Wieczorek,[†] André Dallmann,[§] Zdravko Kochovski,[‡] and Hans G. Börner*[,†]

[†]Laboratory for Organic Synthesis of Functional Systems and [§]Department of Chemistry, Humboldt-Universität zu Berlin, Brook-Taylor-Str. 2, D-12489 Berlin, Germany

[‡]Soft Matter and Functional Materials, Helmholtz-Zentrum Berlin für Materialien und Energie, Hahn-Meitner-Platz 1, Berlin, Germany

Supporting Information

ABSTRACT: Amphiphilic drug formulation additives based on palmitic acid-modified poly(ethylene glycol) (Pal-PEG) are combined with a tailored drug binding peptide that is positioned at the hydrophobic−hydrophilic interface. The peptide originates from combinatorial selection and enables precise modulation of the drug release profiles. While Pal provides a cost-effective reservoir for drug storage, the PEG realizes solubility and shielding. The precision additives reach high payloads close to 1:1, rendering a photosensitizer water-soluble and providing adjustable drug activation kinetics by fine-tuning the peptide interface layer.

Expenses for pharmacological drug development of new entities are constantly rising,[1] as the vast majority of structures fail on their way to approval.[2] Progressively, emphasis is set on small organic molecule drugs[3,4] and with this, low water solubility emerges as one of the key problems, resulting in poor bioavailability and undesirable pharmaceutical profiles.[5,6] To improve solubility of small molecule compounds and reduce failure risks, the development of delivery systems and formulation additives has been the center of attention.[7−13] Amphiphilic macromolecules comprise a successfully applied class of additives, improving solubility of hydrophobic drugs.[14−19] Typically, unspecific interactions, e.g., entropy driven hydrophobic contacts are exploited to host the drugs. Recently, peptide-polymer conjugates, which combine monodisperse peptide segments with synthetic polymers, were recognized in the field of precision polymers.[20,21] Peptide-poly(ethylene glycol) (peptide-PEG) conjugates proved capable to render small molecule drugs water soluble.[22−24] These formulation additives provided advanced specificity as the peptide sequences were selected by combinatorial means from large peptide libraries to specifically interact with the drug. This approach was shown for *m*-tetrakis(hydroxyphenyl)-chlorin (*m*-THPC, Foscan), one of the most effective second-generation sensitizers for photodynamic cancer therapy.[25,26]

The payload capacities as well as drug release rates of these peptide−polymer conjugates were strongly sequence dependent and thus both relevant parameters can be adjusted precisely. Nevertheless, the payload was inherently determined by the peptide and an increase was feasible by adapting length or architecture of the cost intensive peptide segment in bioconjugates.[27] For established amphiphilic formulation additives such as Pluronic, the payload scales often with the weight fraction of the hydrophobic segment. Thus, the capacity can be adjusted in a cost-effective manner, but those solubilizers usually lack drug-specific interactions, which are important for tuning drug release profiles.

Here we introduce precision additives for *m*-THPC as a photosensitizer for the photodynamic cancer therapy. The novel additive combines high payload capacity and cost effectiveness of common amphiphilic formulation additives with precise tuneability of peptide-PEG conjugates. This was achieved by integrating a peptide segment into palmitic acid-modified poly(ethylene glycol) (Pal-PEG). By positioning the peptide at the interface between Pal and PEG-block, a cost-effective drug reservoir system was obtained, exhibiting advantages of drug specific interactions for tuning drug release (Figure 1).

One of the most promising peptide-PEG conjugate solubilizers for *m*-THPC exhibited QFFLFFQ as a peptide sequence and a PEG-block of M_n = 3200 g/mol (H_2N-QFFLFFQ-PEG, **PII**).[22] The bioconjugate could be extended via a GG-spacer by an N-terminal amidation with palmitic acid,

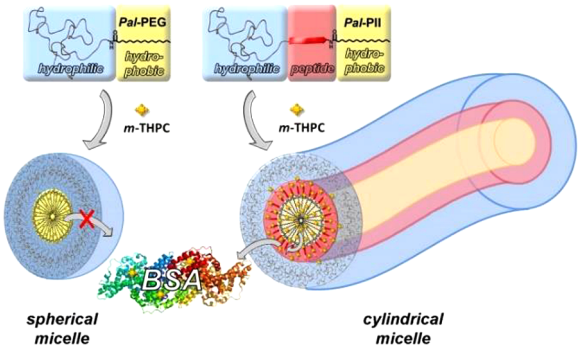

Figure 1. Schematic illustration of the diblock copolymer (**Pal-PEG**) and triblock peptide conjugate (**Pal-PII**) that host *m*-THPC in the cores of self-assembled micellar (**Pal-PEG**) and cylindrical aggregates (**Pal-PII**). Effective transfer of drug molecules to BSA (PDB 3 V03) is mediated through peptide interlayer exclusively present in the **Pal-PII** aggregates.

Received: April 7, 2016
Published: July 11, 2016

DOI: 10.1021/jacs.6b03604
J. Am. Chem. Soc. 2016, 138, 9349−9352

yielding a palmitic acid-peptide-PEG triblock conjugate (**Pal-PII**). **Pal-PII** as well as the diblock references **PII** and **Pal-PEG** were synthesized by a solid phase supported synthesis on PEG preloaded resins (Figure 2 and SI).

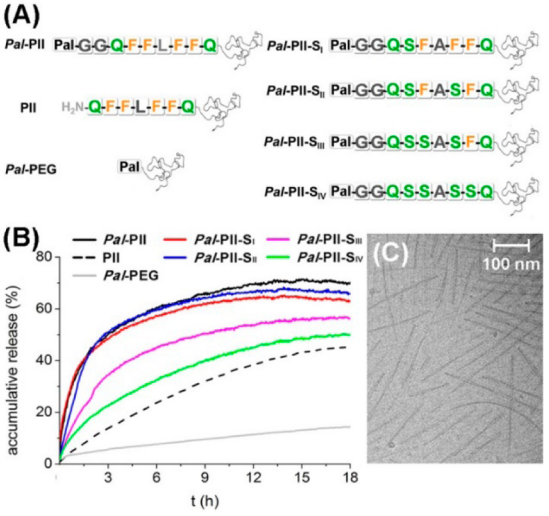

Figure 2. Idealized structure of triblock conjugates and references (A). *m*-THPC trans-solubilization and activation kinetics from *m*-THPC/solubilizer complexes upon BSA addition by fluorescence spectroscopy (B, conditions: λ_{ex} = 417 nm, λ_{em} = 654 nm, 100 μM BSA, [*m*-THPC] = 0.1 μM). Cryo-EM image of *m*-THPC/**Pal-PII** self-assembly to cylindrical micelles (C).

All conjugates and references were readily soluble in water and could be loaded with *m*-THPC through a forced loading procedure (Table S1).[22] The drug payloads were determined by UV−vis spectroscopy, measuring the absorption of *m*-THPC at 650 nm (SI). **Pal-PII** renders *m*-THPC water soluble most effectively. Obviously, the N-terminal modification of peptide-PEG conjugates with palmitic acid significantly enhanced payload capacity. Where **Pal-PII** reached a superior payload of 0.86 mmol drug per mmol conjugate (1:1.2 drug/carrier ratio), the unmodified **PII** solubilized only 0.31 mmol drug per mmol conjugate (1:3.2 drug/carrier ratio).[22] Interestingly, the reference compound **Pal-PEG**, which lacks the peptide segment, solubilized 0.37 mmol *m*-THPC per mmol carrier (1:2.7 drug/carrier ratio) and reached comparable payloads to **PII**. One could speculate that the capacity might be additive based on hydrophobic volume fractions from hydrophobic Pal and peptide sections. This would underline the concept that the drug reservoir does not have to be a cost intensive peptide, but can be formed by an inexpensive hydrophobic segment such as Pal. However, capacity is only one important aspect of a drug solubilizer as is tunable drug release, which certainly requires the peptide for modulation of *m*-THPC activation kinetics.

Dynamic light scattering (DLS) was used to investigate the mode of aggregation and drug solubilization of **Pal-PII** compared to **PII** and **Pal-PEG** (Table S2). It appears that the introduced Pal segment stabilizes the aggregation of **Pal-PII**. This was confirmed by DLS, indicating aggregates for **Pal-PII** prior to and after *m*-THPC loading with comparable hydrodynamic radii of R_h= 43 ± 1 and 41 ± 1 nm, respectively. **PII**, in contrast, exhibited a change of aggregation upon loading.[22] Pure **PII** forms aggregates with R_h= 37 ± 7 nm, which increase to R_h = 165 ± 22 nm after loading. Similar behavior was found for **Pal-PEG**, exhibiting aggregates with R_h= 7 ± 1 nm in the unloaded state and a significant increase toward R_h= 41 ± 1 nm upon loading. It should be noted that due to the more hydrophobic Pal block of **Pal-PII**, more distinct aggregates are found, where drug loading non-dramatically modulates the aggregate sizes.

Considering the molecular dimension of **Pal-PII**, the hydrodynamic radii found by DLS were too large to suggest micellar aggregates. Cryo-electron microscopy (cryo-EM) on solutions of **Pal-PII** prior to and after *m*-THPC loading revealed insight into morphologies and sizes of those nanoformulations. Interestingly, **Pal-PII** formed cylindrical micelles of ∼20 nm in diameter and a few hundred nanometers in length, regardless of drug loading states (Figures 2 and S17). The contrast-rich core of the worm-like structures exhibits a diameter of ∼8 nm, suggesting a corona of ∼2 × 6 nm that might be constituted by well-solvated PEG. These findings are in agreement with the DLS data, indicating no significant increase of the aggregate sizes after drug solubilization. Loading the reference additive **Pal-PEG** with *m*-THPC results in spherical micellar structures with contrast-rich cores of ∼20−30 nm in diameter (Figure S17). Assuming a similar PEG corona as found for the worm-like structures of **Pal-PII**, the sizes of loaded **Pal-PEG** aggregates agree well with the 41 nm found by DLS. It can be anticipated that the hydrophobic Pal segment in both additives drives core formation and aggregate stabilization. The peptide segment, which is only present in **Pal-PII**, might direct the self-assembly in water into anisometric cylindrical micelles either by π-stacking of Phe residues as shown for FFFF-PEG[28] or by increasing the packing parameter of the amphiphile. However, the aggregate morphologies of **Pal-PEG** and **Pal-PII** explain the different behavior of aggregate sizes during *m*-THPC loading. While cylindrical micelles have the possibility to grow exclusively in longitudinal directions and marginal changing interfacial curvature, micellar structures instead have to grow necessarily in size.

The morphology control present in this system seems to be an interesting aspect, as cylindrical micelles have been shown to enable extended *in vivo* circulation times compared to spherical micelles and larger core volumes for drug storage are provided.[1] Thus, the self-assembly behavior of **Pal-PII** can be advantageous over micelle-forming block copolymers like **Pal-PEG**.

The amphiphilic **Pal-PEG** results in the formation of spherical aggregates with PEG shells and hydrophobic Pal cores into which *m*-THPC can be stored due to unspecific interactions. Based on the architecture of the triblock conjugate, cylindrical aggregates are formed by **Pal-PII,** where the more polar peptide segment is probably positioned at the internal interface between core and shell.[29] This would enable the peptide to not only increase the loading capacity by hosting *m*-THPC but, more importantly, also modulate the drug release kinetics as found in the **PII** bioconjugates. STD-NMR spectroscopy exploiting water saturation transfer provided insights into the inner aggregation structure and confirmed the anticipated aggregation model (Figures 1 and S16). In aqueous solutions of *m*-THPC/**Pal-PII** complexes, all resonances of both peptide and PEG are cosaturated upon water saturation prior to acquisition. The characteristic resonances of the Pal segment instead remained unperturbed. This suggests a strong water exposure of the PEG-peptide segment, while Pal is nonhydrated and effectively shielded from water access.

Pal-PII provided high payloads as an *m*-THPC solubilizer. Consequently, the impact of Pal modification on *m*-THPC

DOI: 10.1021/jacs.6b03604
J. Am. Chem. Soc. 2016, 138, 9349−9352

release kinetics was investigated (Figure 2). The high loading of conjugate solubilizers results in almost complete quenching of *m*-THPC fluorescence and singlet oxygen production.[22,30] As previously shown for *m*-THPC/**PII** complexes, the addition of blood plasma model proteins, e.g., albumins (BSA), leads to trans-solubilization of *m*-THPC molecules to BSA, which probably proceeds by a collision-transfer process between the species. This causes monomerization of the sensitizer, resulting in *m*-THPC activation that can be followed by fluorescence spectroscopy at 654 nm.[31] For the photodynamic therapy, it might be advantageous that the photosensitizer is transported in a silent, inactive state to potentially reduce risks during handling and increase shelf lifetimes. However, after application the drug should be activated rapidly, enabling the photodynamic therapy with irradiation to proceed. Comparing the drug activation kinetics from *m*-THPC/**Pal-PII** with those from *m*-THPC/**Pal-PEG** indicated a remarkable acceleration of the *m*-THPC trans-solubilization by the peptide segment and the different morphology. 50% of the drug was activated from *m*-THPC/**Pal-PII** complexes within 3 h and reached a plateau after 12 h, which corresponds to 64% release. In contrast, *m*-THPC/**Pal-PEG** complexes exhibited a strongly retarded activation profile as only 6% and 11% of the overall drug load was activated after 3 and 12 h, respectively. This behavior is consistent with release kinetics found for activation of *m*-THPC from complexes with commonly used formulation additives such as Pluronic F68 or Cremophor ELP (Figure S15).[22] Apparently the slow activation can be correlated to the nonspecific hydrophobic interactions present in these "gold standard" formulation additives to bind and host the *m*-THPC cargo. Comparing the R_h of loaded *m*-THPC/**Pal-PII** and *m*-THPC/**Pal-PEG** complexes prior to those after BSA incubation, some indications are found that trans-solubilization and drug activation proceed via a collision-transfer mechanism. This could be concluded as the hydrodynamic radii of the drug/carrier complexes are increasing after BSA addition (Table S2).

Remarkably, the evolving fluorescence emission of **Pal-PII** solubilized *m*-THPC occurs even in comparison to the reference *m*-THPC/**PII** with a significantly increased rate (Figure 2). This behavior is especially interesting as one would expect a retarded release from **Pal-PII** compared to **PII** since the hydrophobic Pal segments form a nonhydrated core. Obviously, the *m*-THPC binding peptides modulate the interface transfer between hydrophobic Pal and BSA in the aqueous environment analogous to phase transfer catalysts. Furthermore, the larger aggregates found for **PII** upon drug loading decrease the active interface between *m*-THPC/**PII** complexed and BSA molecules, which would explain the slower transfer and drug activation found in the *m*-THPC/**PII** complexes compared to *m*-THPC/**Pal-PII** complexes.

To reveal the effects of the peptide sequence on payload and drug release, a set of triblock conjugates was synthesized, having the same PEG and Pal segments, but differing peptide sequences (cf. SI). Those solubilizers exhibited peptide segments where systematically *m*-THPC affine amino acids have been replaced by weaker binding residues such as Ala and Ser (Figure 2 and SI, **Pal-PII-S$_{I-IV}$**). As expected, the decrease of the maximum *m*-THPC payload follows the reduction in binding residues. Ultimately **Pal-PII-S$_{IV}$**, where all aromatic Phe and hydrophobic Leu residues have been replaced, features a similar payload capacity as **Pal-PEG** (0.36 mmol drug per mmol carrier). This supports the hypothesis that not only the Pal moiety but also the peptide segment contributes to drug storage. However, the drug binding strength appears to be the essential parameter for tuning the *m*-THPC release rates, and this should be precisely adjustable by the peptide sequence. The effect was studied by following the drug activation kinetics of *m*-THPC solubilized with **Pal-PII-S$_{I-IV}$** (Figure 2). Only minor effects were obvious for **Pal-PII-S$_{I+II}$** carrying one and two Ser substitute residues as *m*-THPC activation proceeds comparable to **Pal-PII**. A strong retardation of fluorescence emission development was, however, noticeable for **Pal-PII-S$_{III+IV}$** having three or four *m*-THPC binding residues substituted. For instance, *m*-THPC/**Pal-PII-S$_{IV}$** complexes provide, after 3 h, ∼23% accumulative drug release, where *m*-THPC/**Pal-PII** already showed 50% release. This suggests that the capability of the peptide segment to bind *m*-THPC is essential to act as a phase-transfer shuttle and promote effective drug transfer from a well-loaded Pal core to BSA. Nevertheless, release of the drug from **Pal-PII-S$_{IV}$** is far quicker than for **Pal-PEG**. This shows that by placing an amphiphilic, weak binding peptide at the hydrophobic−hydrophilic interface can modulate release kinetics and overcome retarded drug release of conventional micelles as found for **Pal-PEG**.

In summary, precision formulation additives were developed that combine the advantages of established amphiphilic block copolymer carriers with those of peptide-PEG solubilizers. By positioning a monodispers peptide segment at the hydrophobic−hydrophilic interface of Pal-peptide-PEG, the precision additive rendered *m*-THPC water soluble. The formulation additives provide with the Pal segment a cost-effective reservoir for *m*-THPC, yielding superior payload capacities of 1:1.2 (drug:carrier) compared to peptide-PEG solubilizers. The formation of cylindrical micelles could be proven by cryo-EM imaging, showing no size increase during drug loading. The peptide constituted a precisely tunable phase-transfer segment at the interface, as confirmed by STD-NMR water saturation experiments. The peptide allowed for the modulation of the *m*-THPC transfer kinetics to blood plasma protein models and thereby the adjustment of drug activation kinetics according to requirements of photodynamic cancer therapy. Systematic alteration of the peptide sequence revealed its contributions to *m*-THPC capacity and drug activation. The implementation of a central peptide segment at the interface of amphiphilic block copolymers might offer means to counter drawbacks of established formulation additives that rely on unspecific hydrophobic effects for drug hosting. This could pave the way toward next-generation additives with drug-specific interactions and precise tuneability to provide future perspectives for polymer-based drug delivery systems.

■ ASSOCIATED CONTENT

Supporting Information

The Supporting Information is available free of charge on the ACS Publications website at DOI: 10.1021/jacs.6b03604.

Experimental procedures and analytical data (PDF)

■ AUTHOR INFORMATION

Corresponding Author

*h.boerner@hu-berlin.de

Notes

The authors declare no competing financial interest.

DOI: 10.1021/jacs.6b03604
J. Am. Chem. Soc. 2016, 138, 9349−9352

■ ACKNOWLEDGMENTS

We acknowledge M. Senge (Trinity College Dublin) for *m*-THPC, K. Linkert (HU) for SPPS, F. Hanßke (HU) for DLS, S. Weidner (BAM) for MALDI, and M. Ballauff (HU) for EM. Funding was granted by the European Research Council under the European Union's 7th Framework Program (FP07-13)/ ERC starting grant "Specifically Interacting Polymers" (305064).

■ REFERENCES

(1) Geng, Y.; Dalhaimer, P.; Cai, S.; Tsai, R.; Tewari, M.; Minko, T.; Discher, D. E. *Nat. Nanotechnol.* **2007**, *2*, 249.
(2) DiMasi, J. A.; Hansen, R. W.; Grabowski, H. G. *J. Health Econ.* **2003**, *22*, 151.
(3) Overington, J. P.; Al-Lazikani, B.; Hopkins, A. L. *Nat. Rev. Drug Discovery* **2006**, *5*, 993.
(4) Bleicher, K. H.; Bohm, H.-J.; Muller, K.; Alanine, A. I. *Nat. Rev. Drug Discovery* **2003**, *2*, 369.
(5) Williams, H. D.; Trevaskis, N. L.; Charman, S. A.; Shanker, R. M.; Charman, W. N.; Pouton, C. W.; Porter, C. J. H. *Pharmacol. Rev.* **2013**, *65*, 315.
(6) Di, L.; Fish, P. V.; Mano, T. *Drug Discovery Today* **2012**, *17*, 486.
(7) Allen, T. M.; Cullis, P. R. *Science* **2004**, *303*, 1818.
(8) Lee, C. C.; MacKay, J. A.; Frechet, J. M. J.; Szoka, F. C. *Nat. Biotechnol.* **2005**, *23*, 1517.
(9) Pelegri-O'Day, E. M.; Lin, E.-W.; Maynard, H. D. *J. Am. Chem. Soc.* **2014**, *136*, 14323.
(10) Allen, T. M.; Cullis, P. R. *Adv. Drug Delivery Rev.* **2013**, *65*, 36.
(11) Kopeček, J. *Adv. Drug Delivery Rev.* **2013**, *65*, 49.
(12) Fleige, E.; Quadir, M. A.; Haag, R. *Adv. Drug Delivery Rev.* **2012**, *64*, 866.
(13) Petros, R. A.; DeSimone, J. M. *Nat. Rev. Drug Discovery* **2010**, *9*, 615.
(14) Zhang, F.; Zhang, S.; Pollack, S. F.; Li, R.; Gonzalez, A. M.; Fan, J.; Zou, J.; Leininger, S. E.; Pavía-Sanders, A.; Johnson, R.; Nelson, L. D.; Raymond, J. E.; Elsabahy, M.; Hughes, D. M. P.; Lenox, M. W.; Gustafson, T. P.; Wooley, K. L. *J. Am. Chem. Soc.* **2015**, *137*, 2056.
(15) Synatschke, C. V.; Nomoto, T.; Cabral, H.; Förtsch, M.; Toh, K.; Matsumoto, Y.; Miyazaki, K.; Hanisch, A.; Schacher, F. H.; Kishimura, A.; Nishiyama, N.; Müller, A. H. E.; Kataoka, K. *ACS Nano* **2014**, *8*, 1161.
(16) Peer, D.; Karp, J. M.; Hong, S.; FaroKhzad, O. C.; Margalit, R.; Langer, R. *Nat. Nanotechnol.* **2007**, *2*, 751.
(17) Hill, M. R.; MacKrell, E. J.; Forsthoefel, C. P.; Jensen, S. P.; Chen, M.; Moore, G. A.; He, Z. L.; Sumerlin, B. S. *Biomacromolecules* **2015**, *16*, 1276.
(18) Radowski, M. R.; Shukla, A.; von Berlepsch, H.; Bottcher, C.; Pickaert, G.; Rehage, H.; Haag, R. *Angew. Chem., Int. Ed.* **2007**, *46*, 1265.
(19) Luxenhofer, R.; Han, Y.; Schulz, A.; Tong, J.; He, Z.; Kabanov, A. V.; Jordan, R. *Macromol. Rapid Commun.* **2012**, *33*, 1613.
(20) Lutz, J.-F.; Ouchi, M.; Liu, D. R.; Sawamoto, M. *Science* **2013**, *341*, 1238149.
(21) Börner, H. G. *Macromol. Rapid Commun.* **2011**, *32*, 115.
(22) Wieczorek, S.; Krause, E.; Hackbarth, S.; Röder, B.; Hirsch, A. K. H.; Börner, H. G. *J. Am. Chem. Soc.* **2013**, *135*, 1711.
(23) Hirsch, A. K. H.; Diederich, F.; Antonietti, M.; Börner, H. G. *Soft Matter* **2010**, *6*, 88.
(24) Lawatscheck, C.; Pickhardt, M.; Wieczorek, S.; Grafmüller, A.; Mandelkow, E.; Börner, H. G. *Angew. Chem., Int. Ed.* **2016**, *55*, 8752.
(25) Dolmans, D. E. J. G. J.; Fukumura, D.; Jain, R. K. *Nat. Rev. Cancer* **2003**, *3*, 380.
(26) Senge, M. O.; Brandt, J. C. *Photochem. Photobiol.* **2011**, *87*, 1240.
(27) Wieczorek, S.; Schwaar, T.; Senge, M. O.; Börner, H. G. *Biomacromolecules* **2015**, *16*, 3308.
(28) Castelletto, V.; Hamley, I. W. *Biophys. Chem.* **2009**, *141*, 169.
(29) ten Cate, M. G. J.; Börner, H. G. *Macromol. Chem. Phys.* **2007**, *208*, 124.
(30) Bonnett, R.; Djelal, B. D.; Nguyen, A. *J. Porphyrins Phthalocyanines* **2001**, *5*, 652.
(31) Michael-Titus, A. T.; Whelpton, R.; Yaqub, Z. *Br. J. Clin. Pharmacol.* **1995**, *40*, 594.

DOI: 10.1021/jacs.6b03604
J. Am. Chem. Soc. 2016, 138, 9349−9352